HHS Public Access

Author manuscript

Eur J Pharm Biopharm. Author manuscript; available in PMC 2022 April 01.

Published in final edited form as:

Eur J Pharm Biopharm. 2021 April ; 161: 15–28. doi:10.1016/j.ejpb.2021.01.018.

Applications of nanotechnology in 3D printed tissue engineering scaffolds

Noah Z. Laird[1], **Timothy Acri**[1], **Jaidev L. Chakka**[1], **Juliana Quarterman**[1], **Walla I. Malkawi**[1], **Satheesh Elangovan**[1,2], **Aliasger K. Salem**[1,3]

[1]Department of Pharmaceutical Sciences and Experimental Therapeutics, College of Pharmacy, University of Iowa, Iowa City, IA, USA.

[2]Department of Periodontics, College of Dentistry and Dental Clinics, University of Iowa, Iowa City, IA, USA.

[3]Department of Chemical and Biochemical Engineering, College of Engineering, University of Iowa, Iowa City, IA, USA.

Abstract

Tissue engineering is an interdisciplinary field that aims to combine life sciences and engineering to create therapies that regenerate functional tissue. Early work in tissue engineering mostly used materials as inert scaffolding structures, but research has shown that constructing scaffolds from biologically active materials can help with regeneration by enabling cell-scaffold interactions or release of factors that aid in regeneration. Three-dimensional (3D) printing is a promising technique for the fabrication of structurally intricate and compositionally complex tissue engineering scaffolds. Such scaffolds can be functionalized with techniques developed by nanotechnology research to further enhance their ability to stimulate regeneration and interact with cells. Nanotechnological components, nanoscale textures, and microscale/nanoscale printing can all be incorporated into the manufacture of 3D printed scaffolds. This review discusses recent advancements in the merging of nanotechnology with 3D printed tissue engineering scaffolds, with a focus on applications of nanoscale components, nanoscale texture, and innovative printing techniques and the effects observed *in vitro* and *in vivo*.

1. Cell scaffolds and tissue engineering

Organ failure and loss of tissue function are issues that impact many people across the globe, often reducing their quality of life. In the United States 20 people die each day while awaiting an organ transplant[1]. Tissue and organ dysfunction can be caused by many diseases, including but not limited to kidney failure[2], heart failure[3], and joint degeneration[4,5]. The result is that tissue replacement is desperately needed, and a number of approaches to tissue replacement already exist or are being developed. These alternative therapies include donor organs, artificial mechanical organs[6], xenotransplantation[7], and

tissue engineering approaches[8,9]. The field of tissue engineering is an interdisciplinary union of engineering and life sciences that is working to develop biological substitutes by seeding cells on scaffolds to restore or enhance tissue function[10]. Tissue engineering relies on manipulating cell interactions, regulatory signals, and scaffold materials to precisely restore native tissue structure and function[11,12].

The source of cells used in tissue engineering depends entirely upon the tissue or organ intended to be regenerated and the native regeneration potential of the site to be regenerated. The cells used in tissue engineering can be freshly isolated cells taken from another site and placed directly into the defect site[13,14], cells comprising a 3D tissue assembled or grown *in vitro*[15,16], or simply local cells that are near the defect site and engage in *in situ* tissue regeneration[17]. The signals to which the cells are exposed must be tightly controlled for optimal tissue engineering because these signals can influence tissue formation by affecting cell proliferation, differentiation, migration, and adhesion[18].

Ideal tissue engineering scaffolds are those that imitate the properties of native tissue and are highly porous to enable diffusion of nutrients and migration of cells[19]. An ideal scaffold is composed of biocompatible and biodegradable materials in order to prevent adverse immune reactions and enable full replacement of the scaffold with regenerated tissue[18,20]. Scaffolds should also have mechanical strength such that they are easily handled, withstand the physiological environment into which they will be placed, and have the desired effect on cell growth, adhesion, and differentiation[12,20-23]. The mechanical properties desired in a scaffold can vary widely depending on the tissue and even the subregion of tissue intended to be regenerated. For example, cortical bone tissue carries a compressive strength of ~200MPa while trabecular bone carries a compressive strength of ~2.5MPa[24]

Multiple manufacturing techniques have been utilized for the production of tissue engineering scaffolds, such as fiber bonding, particulate leaching, solvent casting, phase separation, electrospinning, melt molding, fiber mesh assembly, freeze drying, and gas foaming[25-30]. Three dimensional (3D) printing is another manufacturing technique that has shown promise in tissue engineering scaffolds because it allows the scaffolds to have complex, defined shapes that range from the centimeter to nanometer scale. The term 3D printing does not refer to a singular technique, and in fact there are multiple categories of 3D printing that refer to more specific methods by which 3D scaffolds can be printed[31]. Some common 3D printing methods are material extrusion, powder bed fusion, and stereolithography, each of which operate via similar principles but which use different means to produce the final structure. Printing a 3D object involves sequential horizontal layering of a series of layers (or slices) on top of one another[31]. For material extrusion (synonymous with fused deposition modeling, or FDM) each slice is made by extruding material in a pattern slice by slice, creating a stack of slices in the shape of the desired object[31]. Powder bed fusion (synonymous with selective laser sintering, or SLS) uses a different approach where each layer is initially deposited as powder material and then fused together (typically with a binding solution or using a sintering laser) in a specific pattern to create each new slice of the object[31]. For stereolithography the print surface is immersed in polymerizable liquid ink that is selectively cured to create each slice, effectively hardening the liquid ink to erect the object from its liquid surroundings slice by slice[31]. The specific 3D printing

technique to be used often depends on which material the final scaffold is intended to be constructed from since certain materials are only compatible with a specific 3D printing technique. Additionally, the materials compatible with 3D printing manufacturing are not always the most biocompatible and this can limit the use of 3D printing with respect to tissue engineering applications. Also, using 3D printing to manufacture scaffolds can be a time-consuming process relative to non-3D printing techniques, especially when making scaffolds with intricate features and shapes[32]. Despite these issues, scaffolds produced by 3D printing can be highly uniform porous structures, containing multiple materials incorporated into discrete regions, and may also be designed to have a morphology specific to the intended implantation site. As a result of these characteristics, scaffolds produced by 3D printing can be made to mimic the extracellular matrix (ECM) and provide microenvironmental cues that stimulate cells to distribute, differentiate, proliferate, attach, and differentiate to form functional tissue[31]. 3D printed scaffolds have also already been used in clinical studies with varying degrees of success[33,34].

The objective of this review is to highlight the importance of nanoscale features and nanotechnology in relation to 3D printing of scaffolds for tissue engineering (Figure 1). The advantages that such scaffolds are afforded due to nanoscale manipulations will be discussed.

2. Cell-material interactions can be mediated by nanoscale texture and nanotechnological components

The overarching goal of tissue engineering is the creation of viable replacements for damaged tissues and organs[35,36]. Multiple factors contribute to the regenerative potential of a tissue engineering scaffold, including topography, surface composition, porosity, hydrophilicity, size, shape, and mechanical strength[37-39]. Early on in tissue engineering research, investigators believed that scaffolds with microporous topography were simply a support structure for cells and the material's function was to manipulate the growth of cells indirectly by enabling infiltration of cells and facilitating diffusion of nutrients and waste products throughout the volume of the scaffold[35,40]. As a result, the focus of the research from that time was on the materials used and the mechanical properties of scaffolds[35]. More recently, the biological properties of scaffolds have been manipulated to provide synthetic microenvironments conducive for interactions at the cell-scaffold interface, in addition to providing biomolecules that promote cellular functions such as proliferation and differentiation[35,41,42]. The effectiveness of this artificial microenvironment depends upon the scaffold's ability to mimic the native microenvironment[35,38]. The ECM contains growth factors and mediates both cell-cell and cell-substrate interactions, making it a key component of native microenvironments[41]. Evidence suggests that proliferation and differentiation among other functions of cells can be modified by the geometrical restrictions placed by scaffolds on seeded cells[43].

The ECM is a composite of biomolecules produced by the cells that comprise a particular tissue[44]. A typical ECM is a well hydrated nanocomposite which contains a variety of proteins and fibers, including signaling proteins, proteoglycans, reticular fibers, adhesion

proteins, collagen fibers, and elastic fibers many of which contribute to the ECM a measure of rigidity[37,45]. The specific makeup of the ECM depends on a multitude of parameters including the pH, gene expression patterns, applied mechanical forces, the requisite oxygen for proper function[38]. All the constituent parts of the ECM are necessary for maintaining the biological, physical, and mechanical signaling that controls essential cell functions including migration, differentiation, adhesion, migration, apoptosis, polarity, gene expression, proliferation, and tissue morphogenesis[35,37,38,41].

It has been shown that cell migration, signaling, cytoskeleton arrangement, differentiation, and adhesion can all be improved when scaffolds are designed to specifically mimic the native microenvironment[37,38,42,46,47]. Biomimicking scaffolds have demonstrated success in directing cellular behavior and have been investigated as potential regenerative therapies for myriad tissue types, including blood vessels, dentin, cartilage, nerves, bone, skin, and the cornea[37,38,45]. It has been found that the structure of a scaffold directly impacts cell function, and in particular it has been found that scaffolds enhance signaling and function when the topography of the scaffold is closer to that of native ECM[39]. The patterning of such surfaces can even impact cell adhesion, signaling, and lineage differentiation, with mesenchymal stem cells (MSCs) differentiating into either osteoblasts or adipose tissue based upon whether cell adhesion sites are spaced 34 nm apart or 63 nm apart, respectively[39].

The topography of a tissue engineering scaffold is a particularly critical component that facilitates cell function, and as a result a great deal of research has focused on replicating naturally occurring ECM topography[37-39,45]. Tissue engineering matrices that closely replicate surface area and porosity of native ECM at the nanoscale create a microenvironment that has been observed to foster improved cell responses, including proliferation and adhesion[37,38,45]. High surface to volume ratios allow for efficient transport of nutrients and waste products, and scaffold surfaces can be modified at the nanoscale to further enhance function[38,43,45]. Research has shown that a nanofibrous topography is important in precursor cell differentiation towards odontoblasts and osteoblasts in both *in vitro* and *in vivo* settings[38]. The fibrous topography has been found to induce expression of specific signaling molecules that direct cellular differentiation[38].

Nanoscale alterations of a scaffold can also be made by the introduction of nanomaterials into otherwise conventional scaffolds[43]. Such nanomaterials can be used to alter the physical and chemical properties of a scaffold by occluding the native surface and conferring changes in physicochemical properties such as electrical conductivity, mechanical strength, and surface chemistry[43]. The encapsulation of therapeutic proteins and nucleic acids in nanoparticles (NPs) has been shown to assist with stimulating healing in bone tissue engineering applications when these NPs were used to coat scaffolds[48]. For cardiac tissue engineering, carbon nanotubes (CNTs) have been incorporated into scaffolds to increase their electroconductivity[49]. Metallic NPs have also been explored as a potential imaging technique and to confer antimicrobial activity to scaffolds[50].

3. Incorporation of nanomaterials into scaffolds

Nanotechnological components such as nanoclays, NPs, and nanotubes have been used in 3D printed (3DP) tissue engineering scaffolds to increase their functionality[51]. Ceramic NPs and NPs containing biomolecules required for the proper formation of tissue have been included in 3DP scaffolds to enhance their bioactivity. Carbon nanostructures such as CNTs and graphene have been used to make scaffolds electroconductive to enhance their utility in applications that benefit from such electroconductivity, such as in cardiac tissue engineering. This section will describe and summarize (Table 1) various nanomaterials incorporated into 3DP scaffolds for tissue engineering, the ability of nanomaterials to modify scaffold functions, incorporation strategies, and effectiveness in tissue engineering related outcomes.

3.1 Polymeric nanomaterials:

Using polymeric particles as sustained release systems for the delivery of growth factors and biomolecules that enhance tissue regeneration is a ubiquitous technique[52]. Due to the technique's popularity, review articles discussing the fabrication of such particles[53] and their more general applications[54] have been published recently. NPs comprised of poly(lactic-co-glycolic acid) (PLGA) and containing bone morphogenetic protein 2 (BMP-2) were produced by Kim et al.[48] using the double emulsion technique to enhance bone tissue engineering scaffolds regenerative abilities. These particles were immersed in a polycaprolactone (PCL) solution and dip coated onto 3DP hydroxyapatite (HA) scaffolds[48]. The resulting release profile of the loaded BMP-2 resulted in a burst release with 50% of the loaded protein being released over the first 3 days, followed by a steady release of the protein over the next 27 days[48]. The inclusion of the loaded NPs increased alkaline phosphatase (ALP) activity in human mesenchymal stromal cells seeded onto the scaffolds[48]. The nanoparticle-loaded scaffolds yielded 40% bone regeneration in 6 mm rabbit calvarial defects over 8 weeks, while scaffolds lacking NPs and the PCL coating resulted in just 20% bone regeneration over the same time[48]. Another group, Zhu et al., investigated a composite hydrogel containing polyethylene glycol diacrylate (PEGDA) and gel methacrylate (GelMA) embedded with PLGA nanospheres loaded with transforming growth factor β1 (TGF- β1) as a material for cartilage regeneration[55]. Zhu et al. verified, using fluorescent nanospheres, that they were evenly distributed throughout the hydrogel and then analyzed the effect of the TGF- β1-loaded nanospheres on MSC gene expression *in vitro*[55]. They found that the TGF-β1 induced increases in collagen II, aggrecan, and soz-9 expression in the MSCs after 3 weeks[55]. Wei et al. utilized PLGA NPs to deliver insulin-like growth factor-1 to improve cartilage tissue formation outcomes[56]. PCL scaffolds were 3DP, coated with polydopamine, and then coated with the insulin-like growth factor-1 (IGF-1)-loaded NPs. The resulting scaffold demonstrated an initial IGF-1 burst release of 40% over three days and another 40% released over the next 27 days[56]. Both rabbit chondrocytes and BMSCs were seeded on the scaffolds and, with the addition of the IGF-1-loaded NPs, significantly increased cell viability, and expression of SOX-9, type II collagen and aggrecan as compared to scaffolds without NPs. A different polymer, chitosan, was used by Zhang et al. to create NPs via electrostatic binding with plasmid DNA encoding *NELL1* at an amine to phosphate ratio (N:P ratio) of 10[57]. The resulting NPs were combined with bioglass and polyvinyl alcohol (PVA) scaffolds seeded with bone marrow stromal cells (BMSCs) that

were then implanted into rhesus macaque mandibular bone defects and harvested after 12 weeks. The defects were analyzed with micro-computed tomography (μCT) and the scaffolds containing the chitosan particles had 70% bone regeneration while the control had just 55% bone regrowth[57].

In addition to improving connective tissue regeneration, polymeric NPs have been used to supply growth factors for other tissue engineering goals, such as nerve tissue regeneration. Lee et al. conducted a study investigating the promotion of nerve tissue growth with nerve growth factor (NGF)-loaded PLGA NPs incorporated into 3DP PEG hydrogels[58]. They found that inclusion of the NPs resulted in a significant increase in the average neurite length and the total length of neurites formed by rat adrenal medulla cells (PC-12 cell line). They also found a trend towards increased neurite length in primary cortical neurons seeded on scaffolds containing NGF-loaded NPs.

Polymeric NPs have also been investigated to increase electrical conductivity of scaffolds in addition to delivering growth factors. Such electrical activity could be useful in the tissue engineering of electrically active tissues, such as cardiac tissue. Ma et al. created a printable ink by dissolving poly-L-lactic acid (PLLA) in a 1,4-dioxane solution with polypyrrole nanotubes and nanospheres[59]. Their scaffolds were 3DP using a pneumatic extrusion 3D printer with a low temperature, after which the scaffold was lyophilized. They found that the addition of polypyrrole conferred minimal cytotoxicity in comparison to PLLA scaffolds lacking the polypyrrole, and that inclusion of polypyrrole brought the conductivity of the scaffolds to ~$7.5x10^{-5}$S/cm[59].

3.2 Mineral nanomaterials:

Nanomaterials that are derived from minerals, such as silica NPs or hydroxyapatite NPs, can modify the mechanical properties of 3DP scaffolds and provide ions that are necessary for proper tissue formation. These mineral-based nanomaterials can be produced with a variety of techniques such as plasma spraying, milling, and precipitation from solution[46,60]. Investigators have added mineral-based nanomaterials to both the bulk of a 3DP scaffold and to the surface of 3DP scaffolds to modify their properties.

Nanomaterials made from calcium phosphate (CaP) are frequently added to 3DP scaffolds to improve bone tissue engineering outcomes since the mineral component of bone is mostly comprised of the CaP mineral carbonated apatite[61,62]. Wang et al. printed a PLLA scaffold containing CaP NPs and recombinant human BMP-2 on a cryogenic platform that froze the printed material so the finished scaffold was able to be immediately freeze dried[63]. The investigators found that inclusion of the CaP NPs improved the elastic modulus and compressive strength of the 3DP scaffolds from 8.5 to 13 MPa and 0.8 to 1.1MPa, respectively. A trend of improved cell attachment and osteogenic differentiation in scaffolds containing CaP particles alone was suggested, but statistical tests did not indicate significant differences[63]. Another group, Yu et al., used a hydrothermal method to create nanohydroxyapatite (nHA) and mixed it with a poly(ester urea)-based ink to 3DP scaffolds[64]. The scaffolds were produced with 0-40% (w/w) nHA and MC3T3-E1 cells were seeded onto them for *in vitro* analysis of cell viability, gene expression, and production of ALP. Interestingly, the 30% nHA group was the ideal group for osteodifferentiation and cell

viability. Concentrations greater than 30% nHA had reduced cell viability, whereas 30% and lower nHA content either improved cell viability or had no effect. ALP activity was significantly increased after 4 weeks of culture when the nHA content was above 30%, and the expression of both osteocalcin and bone sialoprotein was significantly increased in scaffolds that contained nHA. These studies demonstrate that CaP nanomaterials can be used in 3DP scaffolds for tissue engineering with minimal impact on cell viability while also improving the osteogenicity of the scaffold.

Silicon dioxide (SiO_2) NPs have also been used in bone tissue engineering to increase the osteogenicity of 3DP scaffolds and to improve the minimum possible printing resolution by enhancing the viscosity of gel inks[65,66]. Roopavath et al. produced SiO_2 NPs with a diameter of 64 nm using the Stöber process, then mixed the particles with an alginate gel in varying amounts, and finally manually extruded the resulting gels before crosslinking with calcium chloride[65]. They found that in comparison to the control (0% SiO_2 NPs) the gel containing 5% SiO_2 NPs had an improved compressive modulus (from 32 MPa to 49 MPa), reduced swelling (from 1268% swelling to 990% swelling), and reduced degradation over 72 hours (61% degraded to 55% degraded)[65]. They also found that the viability of umbilical cord MSCs was increased after 7 days of culture and remained above the other experimental groups until day 21. Another mineral used for tissue engineering is zinc oxide, and Cleetus et al. dispersed zinc-oxide NPs in an alginate gel to provide antimicrobial activity and stiffer mechanical properties[67]. Additionally, UV-light shone on the gels stimulated the zinc-oxide NPs to produce free radicals which furthered the antimicrobial activity. Of note the inclusion of zinc oxide NPs was not toxic to mitomycin-C treated STO (MITC-STO) fibroblasts seeded on the gels, suggesting this could be a useful inclusion for wound treatments[67].

3.3 Carbon nanotubes (CNTs):

CNTs have been used to increase the conductivity of 3DP scaffolds to improve their efficacy in cardiac tissue engineering. Various methods are utilized to produce CNTs, including chemical vapor deposition, arc discharge, and laser vaporization, after which they are purified[68]. One property of CNTs that differentiates them from biological agents is that they are highly heat resistant, thus they are able to be incorporated into printable thermoplastic materials. The most common use of CNTs in tissue engineering is for cardiac tissue engineering, however they have also been used for bone and nerve tissue engineering. Ho et al. mixed CNTs (30 nm diameter, 20 μm length) into 3DP scaffolds made from PCL polymer at ratios between 0% and 5% (w/w) to test their application in cardiac tissue engineering[49]. They found that the elastic modulus, conductivity, and maximum load of the scaffolds increased with increasing CNT content. The hardness of the scaffolds they produced was analyzed with nanoindentation, and they found that the hardness of the scaffolds increased slightly when CNTs were included. Viability of H9C2 myoblast cells seeded onto the scaffolds was also investigated, and they found that the presence of CNTs had no impact on the viability of seeded cells[49]. Izadifar et al. took another approach and embedded CNTs within alginate gels, methacrylated collagen gels, and hybrid gels that were printed into scaffolds and then assessed the effect of the inclusion of CNTs on conductivity, cell compatibility, and the mechanical properties of the 3DP scaffolds[69]. They found that the addition of up to 10% CNTs w/w (the highest concentration tested) did not affect the cell

compatibility of the scaffolds, and that the conductivity and mechanical properties were both significantly enhanced. In another approach, a nanoscale printing technique, electrohydrodynamic printing (EHDP), was used by He et al. to print composite scaffolds made from polyethylene oxide, PCL, and CNTs[70]. Cell attachment in the scaffolds containing CNTs was found to be lower when H9C2 cells were seeded onto them, but further investigation showed that those cells that were attached could proliferate and align themselves along the scaffolds[70].

Lee et al. incorporated CNTs into a PEGDA hydrogel ink at concentrations up to 0.1% (w/v) that was then printed into scaffolds designed for nerve tissue engineering [71]. Scaffolds containing CNTs had significantly decreased hydrophilicity yet did not reduce the cell viability of neural stem cells after 14 days in culture. Scaffolds containing CNTs also demonstrated increased average total neurite length (113% increase) over the control scaffolds and seeded cells experienced increased neuronal differentiation gene expression upon electrical stimulation[71]. Huang et al. tested CNTs in scaffolds intended for bone tissue engineering by mixing CNTs with PCL at concentrations of up to 3% (w/v) before subsequent 3D printing into scaffolds whose mechanical strength, cell compatibility, and protein adsorption were tested (Figure 2)[72]. They found that scaffolds containing 3% CNTs (vs scaffolds without CNTs) had higher hardness (0.05 GPa vs 0.04 GPa), elastic moduli (0.65 GPa vs 0.48 GPa), compressive moduli (81 MPa vs 55 MPa), and higher cell viability when seeded with human adipose-derived MSCs. For bone tissue engineering purposes, Liu et al bound single-stranded DNA (ssDNA)-CNT complexes to ammonolyzed 3DP poly(propylene fumarate) (PPF) scaffolds through electrostatic interactions between the ssDNA and the amine groups[73]. The ssDNA reduces the aggregation and the toxicity of the CNTs and the CNTs can consequently enhance the conductivity of the scaffold, allowing for electrical stimulation of the attached cells that has been reported to enhance osteogenesis *in vitro*. With continuous electrical stimulation of seeded MC3T3-E1 cells, ALP, OCN, and OPN were all significantly increased at the 21-day timepoint[73].

3.4 Metallic nanomaterials:

Metal compounds dissolved in solution have been demonstrated to influence cell differentiation when added to tissue engineering scaffolds, however incorporation of metals as NPs can yield different properties and effects[74]. Silver NPs can give scaffolds antimicrobial activity while iron NPs can behave like imaging agents for diagnostics and give otherwise non-magnetic scaffolds magnetic properties. Such metal NPs can be manufactured using physical methods, biological methods, and through wet chemistry. For a more comprehensive overview of metal NPs, the reader is directed to a recent review article specifically on metal NPs by Tan et al[75].

Deng et al. fabricated 3DP scaffolds with polyether ether ketone (PEEK) and coated the scaffolds first with dopamine and then with silver nitrate to create silver NPs on the surface of the scaffold[50]. Upon exposing the scaffolds to *E. coli* and *S. aureus* they found significantly reduced bacterial viability in a 5 mm radius of the scaffold. The researchers also found a slight decrease in cell viability when human osteoblast-like cells (MG-63 cells) were grown on the scaffold. In another study, Buyukhatipoglu et al. loaded magnetic iron

oxide (Fe_2O_3) NPs into alginate gels (2% w/v) by either exposing porcine aortic endothelial cells to the NPs prior to the cells embedment into alginate gel or mixing the cells with alginate gels and then adding in the NPs[76]. The resulting gel mixtures were then printed, and the researchers found that the Fe_2O_3 NPs can be moved both within cells and through the alginate gels by exposing them to an external magnet. The investigators postulated that bioactive molecules could be moved within cells by conjugating them to the Fe_2O_3 NPs. The NPs were also trackable with μCT, which the investigators suggested could be used to track specific biomolecules within cells and scaffolds[76].

Titanium dioxide (TiO_2) NPs were added to PCL scaffolds by Tamjib et al. by solvent casting of a PCL solution that contained the NPs in molds made by 3D printing[77]. Scaffolds that contained the TiO_2 NPs had improved mechanical properties, with their elastic modulus and hardness being superior to that of scaffolds without the NPs. Despite improved mechanical properties, the production of ALP by MC3T3 cells was unaffected by the inclusion of NPs, suggesting that the particles do not significantly impact osteodifferentiation. In a study by Celikkin et al., gold NPs (AuNPs) were embedded into GelMA hydrogel to create a printable ink that could be visualized with μCT[78]. They found that GelMA required the AuNPs in order to be visible using μCT and that the AuNPs did not impact cell viability nor osteoinduction.

4. Adding nanoscale roughness and features to scaffolds

The modification of scaffolds to create nanoscale features and texture is one way that 3DP scaffolds can be made to interact with cells at the nano scale. As described above, research has demonstrated that nanoscale features can guide cellular behaviors to improve regeneration. This section will summarize many approaches to modifying 3DP scaffolds to create these nanoscale features have been investigated, such as degradation, surface modification, and incorporating nanoscale materials (Table 2).

4.1 Nanocomposite scaffolds:

Tissue engineering scaffolds made only from 3DP polymeric materials are often quite smooth after printing. One approach to giving these surfaces nanoscale texture is to incorporate crystalline NPs into the polymer mix, creating a composite material. Tricalcium phosphate (TCP) and HA nanocrystals are popular materials that have been extensively tested as additives to polymer bases to create 3DP tissue engineering scaffolds that have nanotexture. In particular, nHA was able to increase cell viability, cell adhesion, and osteoconduction upon incorporation into polymers for 3DP tissue engineering scaffolds[79-82].

Castro et al. investigated incorporating nHA into a PEG-based hydrogel at a concentration of 60% (wt/wt) that was then investment cast with a 3DP construct[79]. They found that the scaffold containing the nHA increased primary MSC adhesion by 114%, that MSC proliferation increased by 57% after 5 days, that glycosaminoglycan and collagen content indicated enhanced osteogenic differentiation, and that the compressive modulus had increased by 61%. In a parallel study, Castro et al. mixed nHA into a PEG mixture with nanospheres containing growth factors that was then 3DP with a stereolithographic printer[80]. In this study they found that scaffolds containing nHA but not growth factor-loaded

nanospheres had enhanced compressive moduli (increased by 29%) and enhanced primary MSC proliferation (increased by 20% on day 3)[80]. A follow up study was conducted by Zhou et al. on 3DP scaffolds that were similar to those mentioned above but with a biphasic structure[82]. They also found that incorporation of nHA alone enhanced primary MSCs' expression of genes that indicate osteogenic differentiation (collagen I, osteopontin, osteocalcin, Runx-2, alkaline phosphatase), but did not promote chondrogenic differentiation in the primary MSCs. Domingos et al. conducted a study that looked at the importance of nanotexture induced by nHA by comparing microhydroxyapatite (mHA) to nHA in 3DP scaffolds made from PCL[81]. The study showed that mHA addition resulted in a 56% increase in the compressive modulus compared to nHA (217.2 MPa vs 138.8 MPa), while scaffolds containing nHA had improved osteogenic differentiation as indicated by increased cell spreading and higher ALP activity.

4.2 Nanofibrous scaffolds:

Typical ECM often contains a nanofibrous network, and so nanofibers have been of interest in tissue engineering research as they can be used to mimic that network. Electrospinning can be used to create fibers with nanoscale diameters and the technique has been used extensively in tissue engineering constructs, as reviewed elsewhere[83]. In recent work, electrospun fibers have been included in 3DP scaffolds to add the benefits of 3DP scaffolds to the benefits of nanofibers[84-90]. Macroscale 3DP scaffolds that contain nanofibers can confer a uniform alignment of fibers that can guide cell differentiation and the formation of certain cell structures[85,89]. Yeo et al. (2016) found that combining aligned PCL fibers with 3DP PCL scaffolds improved the morphology of seeded myoblasts and the expression of myogenic genes[90]. In particular, the genes for troponin T, MyoD, and myosin heavy chain were all upregulated in the myoblasts seeded onto the aligned fiber scaffolds and the cells were also seen to have changed their morphology from a star shape toward an elongated morphology that closely matched the orientation of the fibers and is associated with myogenic differentiation[90]. In a subsequent study, Yeo et al. (2020) investigated encasing human umbilical vein endothelial cells (HUVECs) and C2C12 cells in fibers via electrospinning a hydrogel cell suspension containing alginate and poly(ethylene oxide) (PEO) onto a 3DP scaffold[91]. They experimented with multiple 3DP scaffolds comprised of PCL, PVA-leached PCL, and PVA-leached collagen, and also co-culturing of electrospun HUVECs with C2C12 myoblast cells. The result was that C2C12 cells seeded onto scaffolds comprised of PVA-leached collagen with electrospun HUVECs encased in alginate/PEO fibers had enhanced myogenic gene expression (myogenin, troponin T, myosin heavy chain, MyoD) while the HUVECs retained high viability after electrospinning[91]. Another group, Touré et al., looked at modifying scaffolds comprised of PCL, poly(glycerol sebacate) (PGS), and bioactive glass (BG) with electrospun fibers made from PCL and PGS[92]. They found that upon inclusion of the electrospun fibers the tensile Young's modulus of their scaffolds increased for all experimental groups (240-310 MPa for scaffolds with fibers vs. 125-280 MPa for scaffolds without fibers)[92]. They also reported good biocompatibility with 3T3 fibroblasts cells, with increases in viability seen on days 1, 2 and 7 for the scaffold containing fibers and 10% BG[92].

4.3 Subtractive methods to induce nanoscale features:

Rather than adding materials and coatings to scaffolds and their constituent materials to yield nanoscale features, some investigators have turned to subtractive techniques to confer nanoscale features to the scaffolds they develop. In particular, etching and incorporation of water-soluble components have proven effective in generating the desired nanoscale features in typically smooth and non-porous scaffolds.

Cheng et al. acid-etched scaffolds they printed via laser sintering titanium-aluminum-vanadium alloy to create nanoscale roughness on the surface of scaffolds[93]. This approach draws on previous research that showed the benefits of rough titanium surfaces in bone tissue engineering applications, with the roughened surfaces enhancing growth factor production and osteoblastic differentiation[94-96]. Cheng et al. designed their titanium-aluminum-vanadium 3DP scaffolds to have differing macroscale porosities and the resulting scaffolds had similar surface roughness, high viability after seeding with osteoblast-like cells (MG-63 cells), though they had differing compressive strengths (from 2579 MPa to 3693 MPa)[93]. In a subsequent study Cheng et al. seeded human MSCs onto their 3DP titanium-aluminum-vanadium scaffolds and similar 2D surfaces[97]. They found that the MSCs on the 3DP scaffolds had higher expression of BMP-2, BMP-4, osteocalcin, and vascular endothelial growth factor (VEGF).

As mentioned above, scaffolds printed from polymeric materials alone often have smooth surfaces, thus researchers have investigated the modification of such scaffolds after printing to give them surface texture. Wang et al. explored treating their 3DP scaffolds comprised of polylactic acid (PLA) with cold atmospheric plasma (CAP) to increase both the roughness and hydrophilicity of their scaffolds[98]. The result was that exposure of their scaffolds to CAP for 5 minutes reduced the hydrophobicity of the scaffolds and increased their surface roughness (R_q) from 120 nm to 27.60 nm. They also found that the proliferation of MSCs and osteoblasts was enhanced in some of the tested CAP treatment groups at most time points and that the CAP treatment increased fibroblast adhesion in some groups tested[98]. Gómez-Cerezo et al. chose a different route for inducing nanoscale texture on their scaffolds and made a blend of water-soluble PVA and mesoporous bioglass (MBG) that was then 3DP to create scaffolds (Figure 3)[99]. The resulting scaffolds were then immersed in phosphate buffered saline (PBS) for varying times to remove the PVA and induce mineralization on the surface of an apatite-like mineral. The result was that scaffolds immersed in PBS for 2 days had increased surface area (from 58.3m^2/g to 186.9m^2/g), increased roughness (from 9.48 nm to 56.74 nm), and enhanced expression of bone-related gene markers (ALP, osteocalcin, Runx2).

5. 3D Printing of scaffolds at the micro and nano scales

Some researchers have taken a different approach to producing 3DP scaffolds with nanoscale features in that they have used 3D printing techniques that can print scaffolds at the micro and nano scales. These printing methods can allow for the design of certain cell-scaffold interactions at the cellular scale to direct differentiation and also enable high levels of control of the overall morphology of scaffolds[100]. Two common approaches to 3D printing at this scale are two-photon polymerization (2PP) and electrohydrodynamic printing

(EHDP). The 2PP method is basically stereolithographic printing at a vastly smaller scale while EHDP is more of a blend of traditional 3D printing techniques merged with electrospinning, and both techniques' applications towards 3DP tissue engineering scaffolds is discussed in the following section (Table 3).

5.1 Electrohydrodynamic printing (EHDP):

Researchers have used EHDP to print defined structures with electrospun fibers for applications that need structures with walls or a mesh with high fidelity to the original design. The method of EHDP is similar overall to the method of electrospinning. In short, a high voltage is applied to a syringe needle containing a polymer solution so the polymer solution jets off from the tip of the needle and dries in flight to create a nanoscale polymer fiber. With typical electrospinning, these strands collect in a disordered fashion on a grounded collection surface, however for EHDP the strands are directed to fabricate specific structures with highly ordered fiber alignment and stacking[101]. EHDP can offer advantages that include fine control over pore diameter, fiber thickness, fiber orientation, and overall porosity[101]. These parameters are tuned by optimizing parameters including nozzle diameter, syringe pressure, printing height, printing speed, applied voltage, and polymer solution viscosity[101,102]. EHDP has also found applications in other fields, such as fluidics and electronics, which has been reviewed elsewhere[101]. For tissue engineering, however, investigators have used EHDP to print 3D scaffolds whose structures are impossible to fabricate with other techniques.

EHDP is particularly useful when making high resolution lattice structures intended to be added to a macroscale scaffold or used as independent scaffolds. One group, Yuan et al., used EHDP to fabricate a PLLA mesh scaffold and looked at cell interactions with scaffolds that had either aligned or random orientations[103]. They seeded the scaffolds with human umbilical arterial smooth muscle cells and found that the cells had greater penetration depth and increased proliferation on scaffolds with aligned fibers compared to the randomly orientated scaffolds. Another group, Kim and Kim, modified the standard EHDP technique by using pins that guide PCL fibers into the correct orientation[104]. The result was a scaffold containing both macroscale PCL fibers and nanoscale PCL fibers that had increased cell alignment, with up-regulated cell metabolism, and cell proliferation after being seeded with MC3T3-E1 cells compared to scaffolds lacking the aligned nanoscale fibers. Bai et al. explored the addition of antibacterial agents to scaffolds fabricated with EHDP by adding roxithromycin (ROX) to PCL/PEG polymers before printing so as to reduce the chance of infection after implanting a scaffold into a bone defect (Figure 4)[105]. They found that the scaffolds were able to induce inhibition zones for both *E. coli* and *S. aureus* while not impacting the viability of MG-63 osteoblast-like cells[105]. Wu et al. tried a different application of EHDP by creating mesh sheets that were rolled into cylinders intended for guided tendon regeneration[106]. These cylindrical scaffolds were seeded with human tenocytes and exhibited enhanced alignment, metabolism, elongation, and collagen I expression. Lei et al. used EHDP to produce a conductive mesh scaffold made with nanoscale conductive fibers fabricated from a conductive polymer blend, poly(3,4-ethylenedioxythiophene)–poly (styrenesulfonate) (PEDOT:PSS) mixed with PEO (PEDOT:PSS-PEO), and microscale PCL fibers[107]. The inclusion of the PEDOT:PSS-PEO

fibers was found to increase adhesion of H9C2 cells, improve the overall conductivity of the scaffolds, and improve both the coordinated beating behavior and the alignment of cardiomyocytes seeded onto the scaffolds.

Investigators have also explored using EHDP to produce walled scaffolds with defined microscale pores[108-111]. Lee and Kim showed that scaffolds made from PEO nanofibers can be fabricated by repeatedly depositing the fibers onto a grounded metal shape, resulting in a walled structure resembling the design[108]. Another group, Wu et al., used EHDP to produce walled scaffolds made from PCL and PCL-chitosan fibers and found that human embryonic stem cells could attach and proliferate on them[111]. Vijayavenkataraman et al. printed conductive scaffolds with EHDP by mixing reduced graphene oxide with PCL solution before printing[109]. They found that the rat medullar cells (PC-12 cell line) they seeded on the scaffolds had enhanced expression of *GAP43* (a neuronal marker) and better proliferation in the conductive scaffolds as compared to the control scaffolds lacking reduced graphene oxide. Wang et al. tried a different approach by fabricating a walled scaffold made from graphene-loaded PCL that also had cores made from PEO that contained dopamine and gelatin[110]. After being submersed in water the PEO would dissolve, allowing the dopamine and gelatin to interact with the PCL to improve its surface properties and leaving the PCL fibers with channels to enhance diffusion and cell infiltration throughout the scaffold. Their scaffolds with the PEO/gelatin/dopamine cores were found to have adequate biocompatibility and improved migration of rat medullar cells (PC-12 cell line) in comparison to scaffolds without the cores.

5.2 Two-photon polymerization (2PP) printing:

As mentioned above, 2PP printing is similar to stereolithographic 3D printing but at a much smaller scale and uses a photocurable polymer that is activated only by the absorption of multiple photons. 2PP printing works by using a focused excitation laser to create a focal point where the curing of the polymer is most efficient because the intensity of light is the highest, making the absorption of the multiple photons required for curing most efficient at the focal point of the laser[112,113]. The spaces above and below the focal point of the excitation laser have a lesser intensity, and since absorption of multiple photons is less efficient in these zones the curing is vastly reduced as the laser is guided along the defined path that creates a single slice of a 3D object[114]. For further information on the topics of multiphoton absorption and 2PP printing the reader is directed towards more in-depth reviews available elsewhere[113,114].

PLA scaffolds made via 2PP printing by Koroleva et al. had their biocompatibility assayed by seeding them with primary rat Schwann (glial) cells and neuronal cells (SH-SY5Y cells)[115]. It was found that the primary Schwann cells could proliferate on the scaffolds while exhibiting expected morphologies and that DNA damage from the scaffold's materials could be reduced by washing the scaffolds in ethanol for 7 days before cell seeding. Another study, by Kuznetsova et al., explored using star-shaped PLA molecules in combination with 2PP and showed that increasing the arm length of the molecules could increase the surface roughness of the resulting scaffolds[116]. The scaffolds with longer PLA molecule arms were also found to enhance the *in vitro* osteogenic differentiation of seeded MSCs and led to CaP

deposition *in vivo*. Rather than fabricate single scaffolds at a time, Maibohm et al. investigated a multi-beam 2PP printing technique in which a repeated pattern was printed over a large area while still retaining near nanoscale resolution[117]. HeLa cells that were seeded onto the completed scaffolds and observed over 120 hours and it was demonstrated that cells could interact with the scaffold in ways that may modify their morphology and that there seemed to be more cells within areas containing 3D structures than in planar areas of the growth surface[117]. In a different approach, Heitz et al. produced 2PP printed 3D lattices with varying pore sizes using a mixture of pentaerythritol triacrylate and bisphenol A glycidyl methacrylate (PETA:BisGMA) and seeded them with primary fibroblast cells before culturing with osteogenic medium to induce differentiation[118]. They reported that when the pores were 35 μm in diameter the pores nearly fill with cells and ECM material and the cells have the best differentiation and collagen type I production. Paun et al. looked into whether a 2PP printed 3D honeycomb scaffold made with multiple layers of vertical microtubes could improve large volume bone tissue regeneration[119]. They found that the MG-63 cells they seeded on the scaffolds had the best penetration and improved osteogenic differentiation (determined by ALP activity) when the layer separation was between 2 μm and 10 μm. Turunen at al. used 2PP printing to create tubular microtowers for 3D cell culture of neuronal cells and found that the microtowers enabled directed neurite generation and long-term culture of the neuronal cells[120].

In all the work described above the materials used were purely polymeric and lacked biomolecules, but researchers have also investigated using structural proteins and other biomolecules in scaffolds produced by 2PP printing. One research group, Kufelt et al., explored adding a major component of ECM, hyaluronic acid, to PEGDA to improve the cell adhesion properties of their scaffolds[121]. They found that the scaffolds were cytotoxic to fibroblasts but not osteoblasts, and that by varying the quantity of hyaluronic acid in the mix they could control the physical properties of the scaffold without affecting cytotoxicity. Prina et al. used 2PP printing to create structures resembling stem cell crypt niches out of GelMA and investigated their effect on the differentiation of primary human limbal epithelial stem cells (hLESCs) seeded onto the scaffolds[122]. They found that cells could grow in the niches and that there was a difference in differentiation of the hLESCs based on where they were physically located on the structure[122]. Engelhardt et al. attempted a different method by using 2PP printing to print polymer-protein hybrid constructs that had the biocompatibility and function of structural proteins in addition to the mechanical strength and stability of polymers[123]. In this case, the polymer structures were printed as supports onto which protein membranes made from GelMA and bovine serum albumin were printed to create hybrid scaffolds. Ovsianikov took a step further and used 2PP printing to print scaffolds made from a gelatin solution containing cells, forgoing any polymeric component in the final scaffolds[124]. They determined that the printing process did result in some cell death after which the surviving cells could replicate and that the cell death was not due to the laser. Chatzinikolaidou et al. incorporated BMP-2 into the base of their 2PP printed scaffolds (a blend of hydrolyzed methacryloxypropyl trimethoxysilane, zirconium isopropoxide, and 2-(dimethylamino)ethyl methacrylate (MAPTMS-ZPO-DMAEMA) in propanol)[125]. They reported that the inclusion of BMP-2 improved ALP and osteocalcin

activity and enhanced calcium and collagen levels in human mesenchymal stem cells seeded onto the scaffolds as compared to the control which lacked BMP-2.

Maggi et al. investigated a different method of scaffold formation, with 2PP printing being used to generate 3 types of 3D nanolattices: 1) sputter coated with TiO_2 and plasma etched ; sputter coated with 2) tungsten (W) or 3) titanium (Ti) followed by a TiO_2 coating[126]. They assayed which scaffold conformation and material combination resulted in the greatest mechanosensitive response and the largest mineral deposition by analyzing fluorescent actin staining and the amount of mineral deposited onto the scaffolds. The results were that osteoblasts (SAOS-2 cell line) had more actin and deposited more mineral when they were seeded on the less stiff nanolattices than when they were seeded on more stiff nanolattices. The potential for 2PP 3DP scaffolds to perform as multifunctional drug release and cell scaffold systems was investigated by Do et al. in their study in which they analyzed the release of their model drug, rhodamine B, from scaffolds made with poly(ethylene glycol) dimethacrylate (PEGDMA)[127]. They found that release of the model drug was tunable by adjusting the strand diameter and pore size of their mesh scaffold and that the scaffolds had no observable cytotoxicity on bone marrow stromal cells, induced pluripotent stem cells, or HEK 293T cells.

6. Future Research Areas and Conclusion

Based on reported findings it is clear that nanotechnological components and nanoscale features can improve the tissue regenerative efficacy of 3DP scaffolds intended for a variety of tissues. However, thus far research on this topic has been mostly simple addition of singular features or additives and there is a lack of studies directly comparing different methods or exploring possible synergies induced by combining multiple methods. Such studies could explore loading multiple nanoparticle treatments into scaffolds to combine antibacterial effects with those that enhance tissue regeneration, or utilizing controlled release properties of polymeric NPs to temporally control the release of specific growth factors. Alternate methods of treating seeded cells with growth factors could be explored as well, for example direct loading of protein growth factors could be replaced with gene activation techniques in which local expression of those growth factors is induced. Gene-activation systems have already been investigated in other tissue engineering studies, but thus far the gene-activation of 3DP scaffolds is under-explored[128-130]. Modification of macroscale scaffolds to confer nanoscale features is an important step in improving the inherent regenerative ability of scaffolds, as has been demonstrated by the works described above. However, other modifications of scaffolds are more pressing in terms of improving overall tissue regeneration of an implanted macroscale scaffold, namely modifying scaffolds to contain vascular structures to perfuse large volumes of regenerated tissue. Modifying the nanotexture of scaffolds is still important in guiding the differentiation of local cells and optimizing the regeneration of tissues, but its potential will be squandered if the issue of vascularization of large scaffolds is not resolved. For micro/nanoscale printing, there has been progress in terms of reducing the minimum resolution of prints and utilizing these printing techniques to produce scaffolds that are able to replicate some aspects of tissue microenvironments, but in most cases the smallest printable features on scaffolds are in the microscale range rather than the nanoscale range. Additionally, the materials used for these

printing techniques often have poor biocompatibility as compared to materials able to be printed at the macroscale. There is a need for the development of ever more refined printing techniques that can enable truly nanoscale printing with materials that are not only biocompatible, but also are able to guide cells in their regeneration of tissue.

Acknowledgements:

This research was supported by a grant from the Lyle and Sharon Bighley Chair of Pharmaceutical Sciences and the Holden Comprehensive Cancer Center (National Cancer Institute of the National Institutes of Health under Award Number P30CA086862).

References:

1. Levi M 50th ACBTSA Meeting Summary, https://www.hhs.gov/oidp/advisory-committee/blood-tissue-safety-availability/meeting-summary/2019-04-15/index.html (2019).
2. Moscalu R, Smith AM & Sharma HL Diseases that can be cured only by organ donations. Arch. Clin. Cases 2, 2015-2(4):182–197 (2015).
3. Martins AM et al. Electrically conductive chitosan/carbon scaffolds for cardiac tissue engineering. Biomacromolecules 15, 635–643 (2014). [PubMed: 24417502]
4. Acri TM et al. Tissue Engineering for the Temporomandibular Joint. Adv. Healthc. Mater 8, e1801236 (2019). [PubMed: 30556348]
5. Makris EA, Gomoll AH, Malizos KN, Hu JC & Athanasiou KA Repair and tissue engineering techniques for articular cartilage. Nat. Rev. Rheumatol 11, 21–34 (2015). [PubMed: 25247412]
6. Love B Chapter 14 - Artificial Organs, in *Biomaterials* (ed. Love B) 337–360 (Academic Press, 2017). doi:10.1016/B978-0-12-809478-5.00014-6.
7. Shimizu A et al. Thrombotic Microangiopathy Associated with Humoral Rejection of Cardiac Xenografts from α1,3-Galactosyltransferase Gene-Knockout Pigs in Baboons. Am. J. Pathol 172, 1471–1481 (2008). [PubMed: 18467706]
8. Chong JJH et al. Human embryonic-stem-cell-derived cardiomyocytes regenerate non-human primate hearts. Nature 510, 273–277 (2014). [PubMed: 24776797]
9. Moon KH, Ko IK, Yoo JJ & Atala A Kidney diseases and tissue engineering. Methods 99, 112–119 (2016). [PubMed: 26134528]
10. Langer R & Vacanti J Tissue engineering. Science 260, 920 (1993). [PubMed: 8493529]
11. Barsotti MC, Felice F, Balbarini A & Stefano RD Fibrin as a scaffold for cardiac tissue engineering. Biotechnol. Appl. Biochem 58, 301–310 (2011). [PubMed: 21995533]
12. Courtney T, Sacks MS, Stankus J, Guan J & Wagner WR Design and analysis of tissue engineering scaffolds that mimic soft tissue mechanical anisotropy. Biomaterials 27, 3631–3638 (2006). [PubMed: 16545867]
13. Gao C et al. Mesenchymal stem cell transplantation to promote bone healing. J. Orthop. Res. Off. Publ. Orthop. Res. Soc 30, 1183–1189 (2012).
14. Ryan EA et al. Clinical Outcomes and Insulin Secretion After Islet Transplantation With the Edmonton Protocol. Diabetes 50, 710–719 (2001). [PubMed: 11289033]
15. Daly AC, Sathy BN & Kelly DJ Engineering large cartilage tissues using dynamic bioreactor culture at defined oxygen conditions. J. Tissue Eng 9, (2018).
16. Haack-Sørensen M et al. Development of large-scale manufacturing of adipose-derived stromal cells for clinical applications using bioreactors and human platelet lysate. Scand. J. Clin. Lab. Invest 78, 293–300 (2018). [PubMed: 29661028]
17. Liu M, Nakasaki M, Shih Y-RV & Varghese S Effect of age on biomaterial-mediated in situ bone tissue regeneration. Acta Biomater. 78, 329–340 (2018). [PubMed: 29966759]
18. Murphy CM, O'Brien FJ, Little DG & Schindeler A Cell-scaffold interactions in the bone tissue engineering triad. Eur. Cell. Mater 26, 120–132 (2013). [PubMed: 24052425]
19. Yang S, Leong KF, Du Z & Chua CK The design of scaffolds for use in tissue engineering. Part I. Traditional factors. Tissue Eng. 7, 679–689 (2001). [PubMed: 11749726]

20. Haugh MG, Murphy CM, McKiernan RC, Altenbuchner C & O'Brien FJ Crosslinking and mechanical properties significantly influence cell attachment, proliferation, and migration within collagen glycosaminoglycan scaffolds. Tissue Eng. Part A 17, 1201–1208 (2011). [PubMed: 21155630]
21. Grover CN, Cameron RE & Best SM Investigating the morphological, mechanical and degradation properties of scaffolds comprising collagen, gelatin and elastin for use in soft tissue engineering. J. Mech. Behav. Biomed. Mater 10, 62–74 (2012). [PubMed: 22520419]
22. Murphy CM, Matsiko A, Haugh MG, Gleeson JP & O'Brien FJ Mesenchymal stem cell fate is regulated by the composition and mechanical properties of collagen–glycosaminoglycan scaffolds. J. Mech. Behav. Biomed. Mater 11, 53–62 (2012). [PubMed: 22658154]
23. Zhu Y, Dong Z, Wejinya UC, Jin S & Ye K Determination of mechanical properties of soft tissue scaffolds by atomic force microscopy nanoindentation. J. Biomech 44, 2356–2361 (2011). [PubMed: 21794867]
24. Morgan EF, Unnikrisnan GU & Hussein AI Bone Mechanical Properties in Healthy and Diseased States. Annu. Rev. Biomed. Eng 20, 119–143 (2018). [PubMed: 29865872]
25. Kheradmandi M, Vasheghani-Farahani E, Ghiaseddin A & Ganji F Skeletal muscle regeneration via engineered tissue culture over electrospun nanofibrous chitosan/PVA scaffold. J. Biomed. Mater. Res. A 104, 1720–1727 (2016). [PubMed: 26945909]
26. Liao C-J et al. Fabrication of porous biodegradable polymer scaffolds using a solvent merging/particulate leaching method. J. Biomed. Mater. Res 59, 676–681 (2002). [PubMed: 11774329]
27. Mikos AG et al. Preparation of poly(glycolic acid) bonded fiber structures for cell attachment and transplantation. J. Biomed. Mater. Res 27, 183–189 (1993). [PubMed: 8382203]
28. Mooney DJ, Baldwin DF, Suh NP, Vacanti JP & Langer R Novel approach to fabricate porous sponges of poly(d,l-lactic-co-glycolic acid) without the use of organic solvents. Biomaterials 17, 1417–1422 (1996). [PubMed: 8830969]
29. Schugens Ch., Maquet V, Grandfils C, Jerome R & Teyssie Ph. Biodegradable and macroporous polylactide implants for cell transplantation: 1. Preparation of macroporous polylactide supports by solid-liquid phase separation. Polymer 37, 1027–1038 (1996).
30. Kwak S, Haider A, Gupta KC, Kim S & Kang I-K Micro/Nano Multilayered Scaffolds of PLGA and Collagen by Alternately Electrospinning for Bone Tissue Engineering. Nanoscale Res. Lett 11, 323 (2016). [PubMed: 27376895]
31. Do A-V, Khorsand B, Geary SM & Salem AK 3D Printing of Scaffolds for Tissue Regeneration Applications. Adv. Healthc. Mater 4, 1742–1762 (2015). [PubMed: 26097108]
32. Hribar KC, Soman P, Warner J, Chung P & Chen S Light-assisted direct-write of 3D functional biomaterials. Lab. Chip 14, 268–275 (2014). [PubMed: 24257507]
33. Hasan S et al. Migration of a novel 3D-printed cementless versus a cemented total knee arthroplasty: two-year results of a randomized controlled trial using radiostereometric analysis. Bone Jt. J 102-B, 1016–1024 (2020).
34. Patel V et al. Prospective Trial of Sacroiliac Joint Fusion Using 3D-Printed Triangular Titanium Implants. Med. Devices Auckl. NZ 13, 173–182 (2020).
35. Dvir T, Timko BP, Kohane DS & Langer R Nanotechnological strategies for engineering complex tissues. Nat. Nanotechnol 6, 13–22 (2011). [PubMed: 21151110]
36. Singh D, Singh D & Han SS 3D Printing of Scaffold for Cells Delivery: Advances in Skin Tissue Engineering. Polymers 8, 19 (2016).
37. Mansouri N & Bagheri S The influence of topography on tissue engineering perspective. Mater. Sci. Eng. C Mater. Biol. Appl 61, 906–921 (2016). [PubMed: 26838922]
38. Rahman SU et al. Fibrous Topography-Potentiated Canonical Wnt Signaling Directs the Odontoblastic Differentiation of Dental Pulp-Derived Stem Cells. ACS Appl. Mater. Interfaces 10, 17526–17541 (2018). [PubMed: 29741358]
39. Viswanathan P et al. 3D surface topology guides stem cell adhesion and differentiation. Biomaterials 52, 140–147 (2015). [PubMed: 25818420]
40. Tsang KY, Cheung MCH, Chan D & Cheah KSE The developmental roles of the extracellular matrix: beyond structure to regulation. Cell Tissue Res. 339, 93 (2009). [PubMed: 19885678]

41. Discher DE, Mooney DJ & Zandstra PW Growth factors, matrices, and forces combine and control stem cells. Science 324, 1673–1677 (2009). [PubMed: 19556500]
42. Murugan R & Ramakrishna S Nano-featured scaffolds for tissue engineering: a review of spinning methodologies. Tissue Eng. 12, 435–447 (2006). [PubMed: 16579677]
43. Krishna L et al. Nanostructured scaffold as a determinant of stem cell fate. Stem Cell Res. Ther 7, (2016).
44. Brown BN et al. Surface characterization of extracellular matrix scaffolds. Biomaterials 31, 428–437 (2010). [PubMed: 19828192]
45. Rahman SU, Nagrath M, Ponnusamy S & Arany PR Nanoscale and Macroscale Scaffolds with Controlled-Release Polymeric Systems for Dental Craniomaxillofacial Tissue Engineering. Mater. Basel Switz 11, (2018).
46. Shin K, Acri T, Geary S & Salem AK Biomimetic Mineralization of Biomaterials Using Simulated Body Fluids for Bone Tissue Engineering and Regenerative Medicine. Tissue Eng. Part A 23, 1169–1180 (2017). [PubMed: 28463603]
47. Singh D, Singh D, Zo S & Han SS Nano-biomimetics for nano/micro tissue regeneration. J. Biomed. Nanotechnol 10, 3141–3161 (2014). [PubMed: 25992433]
48. Kim BS, Yang SS & Kim CS Incorporation of BMP-2 nanoparticles on the surface of a 3D-printed hydroxyapatite scaffold using an ε-polycaprolactone polymer emulsion coating method for bone tissue engineering. Colloids Surf. B Biointerfaces 170, 421–429 (2018). [PubMed: 29957531]
49. Ho CMB et al. 3D Printed Polycaprolactone Carbon Nanotube Composite Scaffolds for Cardiac Tissue Engineering. Macromol. Biosci 17, 1600250 (2017).
50. Deng L, Deng Y & Xie K AgNPs-decorated 3D printed PEEK implant for infection control and bone repair. Colloids Surf. B Biointerfaces 160, 483–492 (2017). [PubMed: 28992487]
51. Bouguéon G, Kauss T, Dessane B, Barthélémy P & Crauste-Manciet S Micro- and nano-formulations for bioprinting and additive manufacturing. Drug Discov. Today 24, 163–178 (2019). [PubMed: 30391204]
52. Hong L et al. Effects of glucocorticoid receptor small interfering RNA delivered using poly lactic-co-glycolic acid microparticles on proliferation and differentiation capabilities of human mesenchymal stromal cells. Tissue Eng. Part A 18, 775–784 (2012). [PubMed: 21988716]
53. Braz AL & Ahmed I Manufacturing processes for polymeric micro and nanoparticles and their biomedical applications. Bioeng. *2017 Vol* 4 Pages 46–72 (2017) doi:10.3934/bioeng.2017.1.46.
54. Sahai N, Ahmad N & Gogoi M Nanoparticles Based Drug Delivery for Tissue Regeneration Using Biodegradable Scaffolds: a Review. Curr. Pathobiol. Rep 6, 219–224 (2018).
55. Zhu W et al. 3D bioprinting mesenchymal stem cell-laden construct with core–shell nanospheres for cartilage tissue engineering. Nanotechnology 29, 185101 (2018). [PubMed: 29446757]
56. Wei P et al. IGF-1-releasing PLGA nanoparticles modified 3D printed PCL scaffolds for cartilage tissue engineering. Drug Deliv. 27, 1106–1114 (2020). [PubMed: 32715779]
57. Zhang J et al. Tissue engineering using 3D printed nano-bioactive glass loaded with NELL1 gene for repairing alveolar bone defects. Regen. Biomater 5, 213–220 (2018). [PubMed: 30094060]
58. Lee SJ et al. Development of Novel 3-D Printed Scaffolds With Core-Shell Nanoparticles for Nerve Regeneration. IEEE Tram. Biomed. Eng 64, 408–418 (2017).
59. Ma C et al. 3D Printing of Conductive Tissue Engineering Scaffolds Containing Polypyrrole Nanoparticles with Different Morphologies and Concentrations. Mater. Basel Switz 12, (2019).
60. Okada M & Furuzono T Hydroxylapatite nanoparticles: fabrication methods and medical applications. Sci. Technol. Adv. Mater 13, (2012).
61. Trombetta R, Inzana JA, Schwarz EM, Kates SL & Awad HA 3D Printing of Calcium Phosphate Ceramics for Bone Tissue Engineering and Drug Delivery. Ann. Biomed. Eng 45, 23–44 (2017). [PubMed: 27324800]
62. Babilotte J et al. 3D printed polymer–mineral composite biomaterials for bone tissue engineering: Fabrication and characterization. J. Biomed. Mater. Res. B Appl. Biomater 107, 2579–2595 (2019). [PubMed: 30848068]

63. Wang C, Zhao Q & Wang M Cryogenic 3D printing for producing hierarchical porous and rhBMP-2-loaded Ca-P/PLLA nanocomposite scaffolds for bone tissue engineering. Biofabrication 9, 025031 (2017). [PubMed: 28589918]
64. Yu J, Xu Y, Li S, Seifert GV & Becker ML Three-Dimensional Printing of Nano Hydroxyapatite/Poly(ester urea) Composite Scaffolds with Enhanced Bioactivity. Biomacromolecides 18, 4171–4183 (2017).
65. Roopavath UK, Soni R, Mahanta U, Deshpande AS & Rath SN 3D printable Si02 nanoparticle ink for patient specific bone regeneration. RSC Adv. 9, 23832–23842 (2019).
66. Yang X et al. The stimulatory effect of silica nanoparticles on osteogenic differentiation of human mesenchymal stem cells. Biomed. Mater 12, 015001 (2016). [PubMed: 27910816]
67. Cleetus CM et al. Alginate Hydrogels with Embedded ZnO Nanoparticles for Wound Healing Therapy. Int. J. Nanomedicine 15, 5097–5111 (2020). [PubMed: 32764939]
68. Jahanshahi M & Kiadehi AD Fabrication, Purification and Characterization of Carbon Nanotubes: Arc-Discharge in Liquid Media (ADLM). Synth. Appl. Carbon Nanotab. Their Compos. (2013) doi:10.5772/51116.
69. Izadifar M, Chapman D, Babyn P, Chen X & Kelly ME UV-Assisted 3D Bioprinting of Nanoreinforced Hybrid Cardiac Patch for Myocardial Tissue Engineering. Tissue Eng. Part C Methods 24, 74–88 (2018). [PubMed: 29050528]
70. He J, Xu F, Dong R, Guo B & Li D Electrohydrodynamic 3D printing of microscale poly (ε-caprolactone) scaffolds with multi-walled carbon nanotubes. Biofabrication 9, 015007 (2017). [PubMed: 28052044]
71. Lee S-J et al. 3D printing nano conductive multi-walled carbon nanotube scaffolds for nerve regeneration. J. Neural Eng 15, 016018 (2018). [PubMed: 29064377]
72. Huang B et al. Fabrication and characterisation of 3D printed MWCNT composite porous scaffolds for bone regeneration. Mater. Sci. Eng C 98, 266–278 (2019).
73. Liu X et al. 3D-printed scaffolds with carbon nanotubes for bone tissue engineering: Fast and homogeneous one-step functionalization. Acta Biomater. 111, 129–140 (2020). [PubMed: 32428680]
74. D'Mello S et al. Incorporation of copper into chitosan scaffolds promotes bone regeneration in rat calvarial defects. J. Biomed. Mater. Res. B Appl. Biomater 103, 1044–1049 (2015). [PubMed: 25230382]
75. Tan H-L, Teow S-Y & Pushpamalar J Application of Metal Nanoparticle–Hydrogel Composites in Tissue Regeneration. Bioengineering 6, 17 (2019).
76. Buyukhatipoglu K, Chang R, Sun W & Clyne AM Bioprinted Nanoparticles for Tissue Engineering Applications. Tissue Eng. Part C Methods 16, 631–642 (2009).
77. Tamjid E et al. Tissue growth into three-dimensional composite scaffolds with controlled micro-features and nanotopographical surfaces. J. Biomed. Mater. Res. A 101, 2796–2807 (2013). [PubMed: 23463703]
78. Celikkin N, Mastrogiacomo S, Walboomers XF & Swieszkowski W Enhancing X-ray Attenuation of 3D Printed Gelatin Methacrylate (GelMA) Hydrogels Utilizing Gold Nanoparticles for Bone Tissue Engineering Applications. Polymers 11, (2019).
79. Castro NJ, Patel R & Zhang LG Design of a Novel 3D Printed Bioactive Nanocomposite Scaffold for Improved Osteochondral Regeneration. Cell. Mol. Bioeng 8, 416–432 (2015). [PubMed: 26366231]
80. Castro NJ, O'Brien J & Zhang LG Integrating biologically inspired nanomaterials and table-top stereolithography for 3D printed biomimetic osteochondral scaffolds. Nanoscale 7, 14010–14022 (2015). [PubMed: 26234364]
81. Domingos M, Gloria A, Coelho J, Bartolo P & Ciurana J Three-dimensional printed bone scaffolds: The role of nano/micro-hydroxyapatite particles on the adhesion and differentiation of human mesenchymal stem cells. Proc. Inst. Mech. Eng. [H] 231, 555–564 (2017).
82. Zhou X et al. 3D Printed scaffolds with hierarchical biomimetic structure for osteochondral regeneration. Nanomedicine Nanotechnol. Biol. Med 19, 58–70 (2019).
83. Pham QP, Sharma U & Mikos AG Electrospinning of Polymeric Nanofibers for Tissue Engineering Applications: A Review. Tissue Eng. 12, 1197–1211 (2006). [PubMed: 16771634]

84. Hauser CAE et al. Natural tri- to hexapeptides self-assemble in water to amyloid β-type fiber aggregates by unexpected α-helical intermediate structures. Proc. Natl. Acad. Sci 108, 1361–1366 (2011). [PubMed: 21205900]

85. Liang D, Hsiao BS & Chu B Functional electrospun nanofibrous scaffolds for biomedical applications. Adv. Drug Deliv. Rev 59, 1392–1412 (2007). [PubMed: 17884240]

86. Loo Y et al. Peptide Bioink: Self-Assembling Nanofibrous Scaffolds for Three-Dimensional Organotypic Cultures. Nano Lett. 15, 6919–6925 (2015). [PubMed: 26214046]

87. Rashad A et al. Coating 3D Printed Polycaprolactone Scaffolds with Nanocellulose Promotes Growth and Differentiation of Mesenchymal Stem Cells. Biomacromolecules 19, 4307–4319 (2018). [PubMed: 30296827]

88. Seow WY, Kandasamy K, Purnamawati K, Sun W & Hauser CAE Thin peptide hydrogel membranes suitable as scaffolds for engineering layered biostructures. Acta Biomater. 88, 293–300 (2019). [PubMed: 30721784]

89. Wang P-Y, Thissen H & Tsai W-B The roles of RGD and grooved topography in the adhesion, morphology, and differentiation of C2C12 skeletal myoblasts. Biotechnol. Bioeng. 109, 2104–2115 (2012). [PubMed: 22359221]

90. Yeo M, Lee H & Kim GH Combining a micro/nano-hierarchical scaffold with cell-printing of myoblasts induces cell alignment and differentiation favorable to skeletal muscle tissue regeneration. Biofabrication 8, 035021 (2016). [PubMed: 27634918]

91. Yeo M & Kim G Micro/nano-hierarchical scaffold fabricated using a cell electrospinning/3D printing process for co-culturing myoblasts and HUVECs to induce myoblast alignment and differentiation. Acta Biomater. 107, 102–114 (2020). [PubMed: 32142759]

92. Touré ABR, Mele E & Christie JK Multi-layer Scaffolds of Poly(caprolactone), Poly(glycerol sebacate) and Bioactive Glasses Manufactured by Combined 3D Printing and Electrospinning. Nanomater. Basel Switz 10, (2020).

93. Cheng A, Humayun A, Cohen DJ, Boyan BD & Schwartz Z Additively Manufactured 3D Porous Ti-6Al-4V Constructs Mimic Trabecular Bone Structure and Regulate Osteoblast Proliferation, Differentiation and Local Factor Production in a Porosity and Surface Roughness Dependent Manner. Biofabrication 6, 045007 (2014). [PubMed: 25287305]

94. Gittens RA et al. The effects of combined micron-/submicron-scale surface roughness and nanoscale features on cell proliferation and differentiation. Biomaterials 32, 3395–3403 (2011). [PubMed: 21310480]

95. Lincks J et al. Response of MG63 osteoblast-like cells to titanium and titanium alloy is dependent on surface roughness and composition. Biomaterials 19, 2219–2232 (1998). [PubMed: 9884063]

96. Martin JY et al. Effect of titanium surface roughness on proliferation, differentiation, and protein synthesis of human osteoblast-like cells (MG63). J. Biomed. Mater. Res 29, 389–401 (1995). [PubMed: 7542245]

97. Cheng A, Cohen DJ, Boyan BD & Schwartz Z Laser-Sintered Constructs with Bioinspired Porosity and Surface Micro/Nano-Roughness Enhance Mesenchymal Stem Cell Differentiation and Matrix Mineralization In Vitro. Calcif. Tissue Int 99, 625–637 (2016). [PubMed: 27501817]

98. Wang M et al. Cold atmospheric plasma (CAP) surface nanomodified 3D printed polylactic acid (PLA) scaffolds for bone regeneration. Acta Biomater. 46, 256–265 (2016). [PubMed: 27667017]

99. Gómez-Cerezo MN, Lozano D, Arcos D, Vallet-Regí M & Vaquette C The effect of biomimetic mineralization of 3D-printed mesoporous bioglass scaffolds on physical properties and in vitro osteogenicity. Mater. Sci. Eng. C Mater. Biol. Appl 109, 110572 (2020). [PubMed: 32228951]

100. Worthington KS, Do A-V, Smith R, Tucker BA & Salem AK Two-Photon Polymerization as a Tool for Studying 3D Printed Topography-Induced Stem Cell Fate. Macromol. Biosci 19, e1800370 (2019). [PubMed: 30430755]

101. Huang Y et al. Electrohydrodynamic direct-writing. Nanoscale 5, 12007–12017 (2013). [PubMed: 24057297]

102. Park J-U et al. High-resolution electrohydrodynamic jet printing. Nat. Mater 6, 782–789 (2007). [PubMed: 17676047]

103. Yuan H et al. Direct printing of patterned three-dimensional ultrafine fibrous scaffolds by stable jet electrospinning for cellular ingrowth. Biofabrication 7, 045004 (2015). [PubMed: 26538110]

104. Kim JI & Kim CS Nanoscale Resolution 3D Printing with Pin-Modified Electrified Inkjets for Tailorable Nano/Macrohybrid Constructs for Tissue Engineering. ACS Appl. Mater. Interfaces 10, 12390–12405 (2018). [PubMed: 29561138]
105. Bai J et al. Melt electrohydrodynamic 3D printed poly (ε-caprolactone)/polyethylene glycol/roxithromycin scaffold as a potential anti-infective implant in bone repair. Int. J. Pharm 576, 118941 (2020). [PubMed: 31881261]
106. Wu Y et al. Mechanically-enhanced three-dimensional scaffold with anisotropic morphology for tendon regeneration. J. Mater. Sci. Mater. Med 27, 115 (2016). [PubMed: 27215211]
107. Lei Q, He J & Li D Electrohydrodynamic 3D printing of layer-specifically oriented, multiscale conductive scaffolds for cardiac tissue engineering. Nanoscale (2019) doi:10.1039/C9NR04989D.
108. Lee M & Kim HY Toward Nanoscale Three-Dimensional Printing: Nanowalls Built of Electrospun Nanofibers. Langmuir 30, 1210–1214 (2014). [PubMed: 24471865]
109. Vijayavenkataraman S, Thaharah S, Zhang S, Lu W & Fuh JYH 3D-Printed PCL/rGO Conductive Scaffolds for Peripheral Nerve Injury Repair. Artif. Organs 43, 515–523 (2018). [PubMed: 30229979]
110. Wang B, Chen X, Ahmad Z, Huang J & Chang M-W 3D electrohydrodynamic printing of highly aligned dual-core graphene composite matrices. Carbon 153, 285–297 (2019).
111. Wu Y et al. Fabrication and evaluation of electrohydrodynamic jet 3D printed polycaprolactone/chitosan cell carriers using human embryonic stem cell-derived fibroblasts. J. Biomater. Appl 31, 181–192 (2016). [PubMed: 27252227]
112. Chakka JL & Salem AK 3D printing in drug delivery systems. J. 3D Print. Med 3, 59–62 (2019). [PubMed: 31258935]
113. Nguyen AK & Narayan RJ Two-photon polymerization for biological applications. Mater. Today 20, 314–322 (2017).
114. Xing J-F, Zheng M-L & Duan X-M Two-photon polymerization microfabrication of hydrogels: an advanced 3D printing technology for tissue engineering and drug delivery. Chem. Soc. Rev 44, 5031–5039 (2015). [PubMed: 25992492]
115. Koroleva A et al. Two-photon polymerization-generated and micromolding-replicated 3D scaffolds for peripheral neural tissue engineering applications. Biofabrication 4, 025005 (2012). [PubMed: 22522957]
116. Kuznetsova D et al. Surface micromorphology of cross-linked tetrafunctional polylactide scaffolds inducing vessel growth and bone formation. Biofabrication 9, 025009 (2017). [PubMed: 28300041]
117. Maibohm C et al. Multi-beam two-photon polymerization for fast large area 3D periodic structure fabrication for bioapplications. Sci. Rep 10, (2020).
118. Heitz J et al. Bone-forming cells with pronounced spread into the third dimension in polymer scaffolds fabricated by two-photon polymerization. J. Biomed. Mater. Res. A 105A, 891–899 (2017).
119. Paun I et al. Laser-direct writing by two-photon polymerization of 3D honeycomb-like structures for bone regeneration. Biofabrication 10, 025009 (2018). [PubMed: 29327690]
120. Turunen S et al. Direct Laser Writing of Tubular Microtowers for 3D Culture of Human Pluripotent Stem Cell-Derived Neuronal Cells. ACS Appl. Mater. Interfaces 9, 25717–25730 (2017). [PubMed: 28697300]
121. Kufelt O, El-Tamer A, Sehring C, Schlie-Wolter S & Chichkov BN Hyaluronic acid based materials for scaffolding via two-photon polymerization. Biomacromolecules 15, 650–659 (2014). [PubMed: 24432740]
122. Prina E et al. Bioinspired Precision Engineering of Three-Dimensional Epithelial Stem Cell Microniches. Adv. Biosyst 4, (2020).
123. Engelhardt S et al. Fabrication of 2D protein microstructures and 3D polymer-protein hybrid microstructures by two-photon polymerization. Biofabrication 3, 025003 (2011). [PubMed: 21562366]
124. Ovsianikov A et al. Laser photofabrication of cell-containing hydrogel constructs. Langmuir 30, 3787–3794 (2013). [PubMed: 24033187]

125. Chatzinikolaidou M et al. Recombinant human bone morphogenetic protein 2 (rhBMP-2) immobilized on laser-fabricated 3D scaffolds enhance osteogenesis. Colloids Surf. B Biointerfaces 149, 233–242 (2017). [PubMed: 27768913]

126. Maggi A, Li H & Greer JR Three-dimensional nano-architected scaffolds with tunable stiffness for efficient bone tissue growth. Acta Biomater. 63, 294–305 (2017). [PubMed: 28923538]

127. Do A-V, Worthington KS, Tucker BA & Salem AK Controlled drug delivery from 3D printed two-photon polymerized poly(ethylene glycol) dimethacrylate devices. Int. J. Pharm 552, 217–224 (2018). [PubMed: 30268853]

128. D'Mello S et al. Bone Regeneration Using Gene-Activated Matrices. AAPS J. 19, 43–53 (2017). [PubMed: 27655418]

129. D'Mello S, Elangovan S & Salem AK FGF2 gene activated matrices promote proliferation of bone marrow stromal cells. Arch. Oral Biol 60, 1742–1749 (2015). [PubMed: 26433191]

130. Khorsand B et al. Regeneration of bone using nanoplex delivery of FGF-2 and BMP-2 genes in diaphyseal long bone radial defects in a diabetic rabbit model. J. Control. Release Off. J. Control. Release Soc 248, 53–59 (2017).

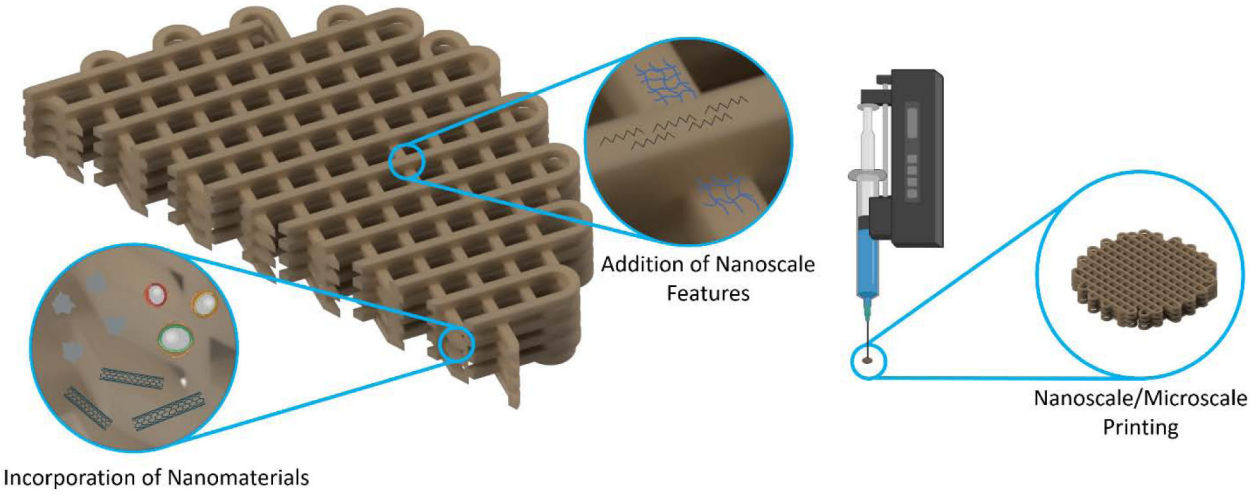

Figure 1:
Methods of merging nanotechnology with 3D printed tissue engineering scaffolds.

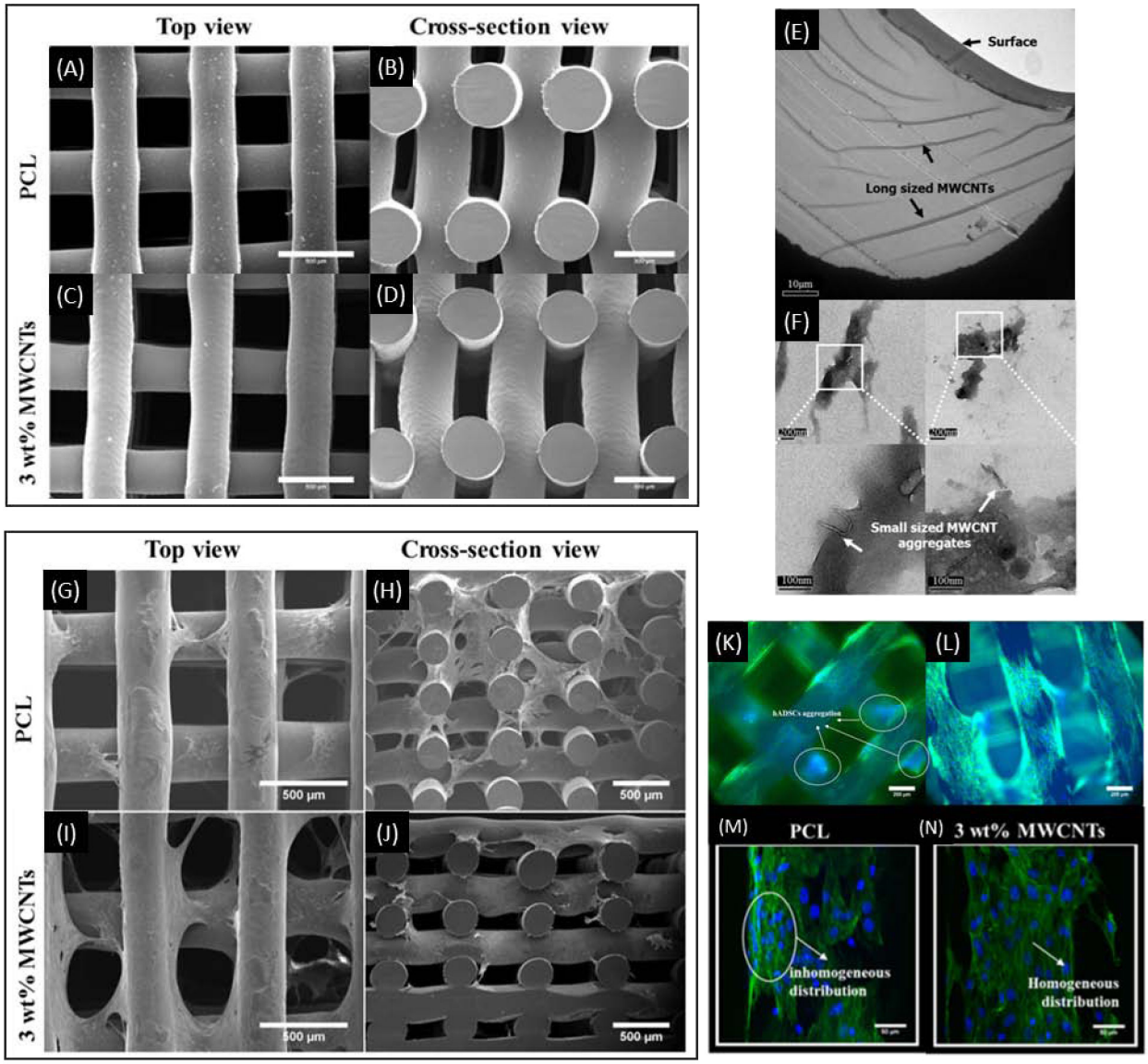

Figure 2:

SEM images of PCL scaffolds lacking CNTs (A, B) and containing 3% CNTs (C, D). TEM images showing extended and aggregated CNTs in the 3% CNT PCL scaffolds (E, F). SEM images of PCL scaffold lacking (G, H) and containing 3% CNTs (I, J) seeded with MSCs and cultured for 14 days. Fluorescence images of PCL scaffolds lacking (K, M) and containing 3% CNTs (L, N) showing cell morphology after MSCs were seeded and cultured for 14 days. **Adapted from Huang et al. 2019.**

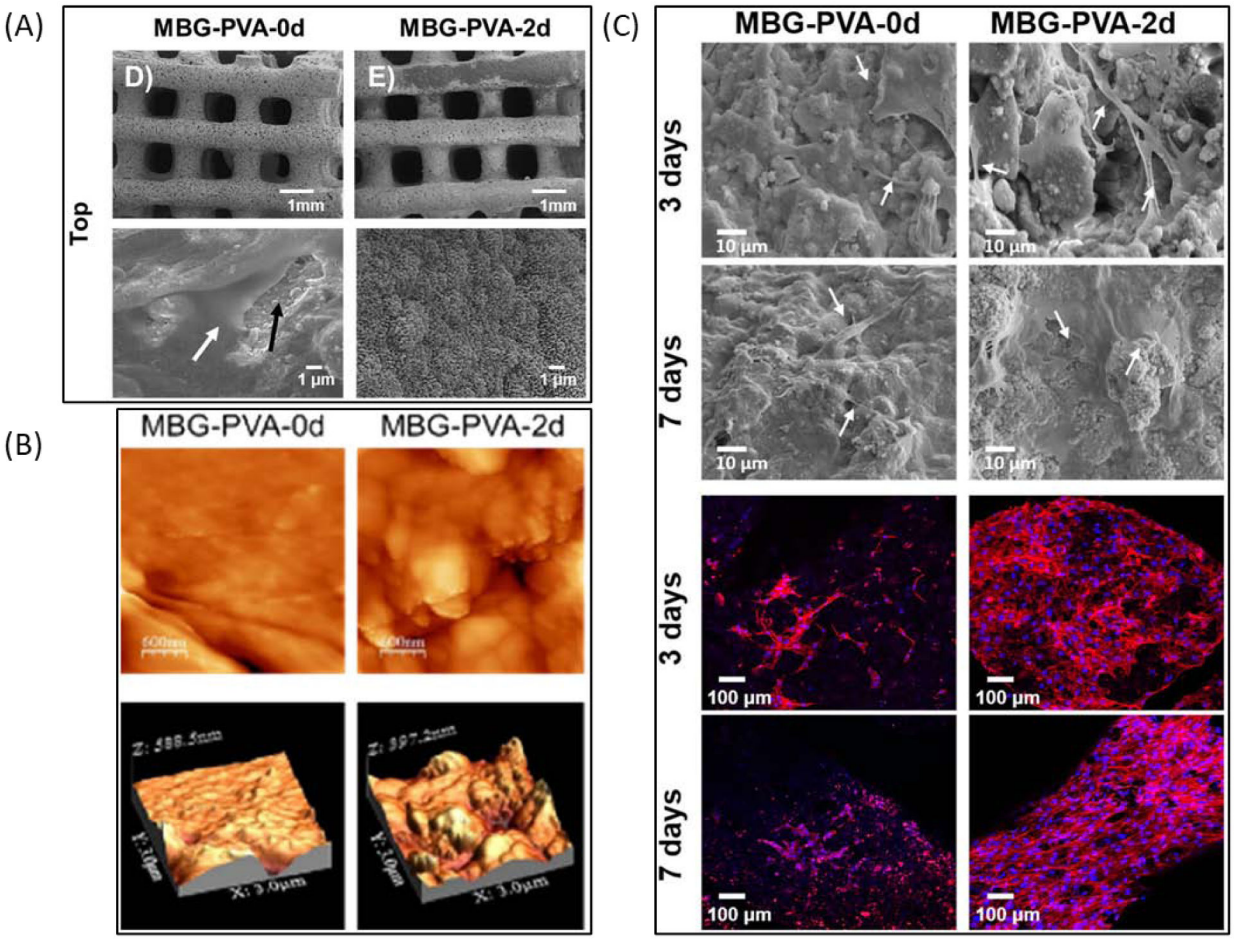

Figure 3:

(A) SEM images of MBG/PVA blend scaffolds after incubation in PBS for 0 or 2 days. (B) Atomic force microscopy images of scaffold surfaces after incubation in PBS for 0 or 2 days. (C) SEM images and fluorescence images of scaffolds seeded with MC3T3-E1 cells and incubated for 3 or 7 days. **Adapted from Gómez-Cerezo et al. 2020.**

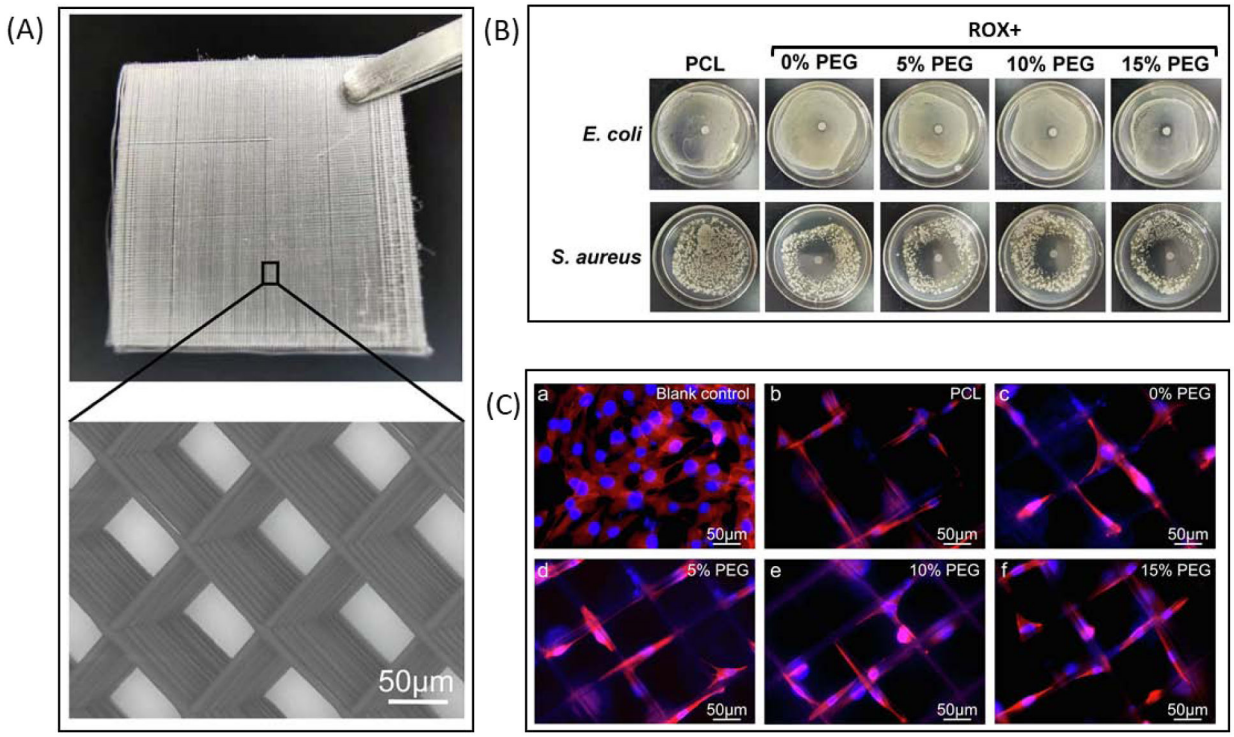

Figure 4:

(A) Photograph and SEM image of fiber mesh printed with EHDP. (B) Photographs of inhibition zones surrounding scaffolds lacking ROX (PCL) or containing ROX (ROX+ groups). (C) Fluorescence images of MG-63 cells seeded onto scaffolds or a 2D control surface. **Adapted from Bai et al. 2020.**

Table 1:

Summary of materials, methods, and results from studies incorporating nanomaterials into 3DP scaffolds

Material(s)	Cell Type/ Animal Model	Method	Results	Citation #
HA scaffold. PCL NPs containing BMP-2	primary MSCs, rabbit model	Dip-coated particles onto scaffold	Improved ALP activity in MSCs; improved bone regeneration in rabbit calvarial defect	44
PEGDA/GelMA scaffold. PLGA nanospheres containing TGF-β1	primary MSCs	Mixed nanospheres with liquid ink before printing	Increased expression of genes associated with chondrogenic differentiation	51
PCL scaffold, polydopamine coating, PLGA NPs containing IGF-1	primary MSCs, primary rabbit chondrocytes	Coated scaffold with polydopamine before co-incubation with NPs	Enhanced cell viability; increased expression of chondrogenic markers	52
PEGDA scaffold, PLGA NPs containing BSA	PC-12 neural cells, primary cortical neurons	Mixed NPs with liquid ink before printing	Increased average neurite length and total neurite length in PC-12 cells	54
PVA and bioglass scaffold, chitosan/pDNA NPs	primary MSCs, rhesus monkey model	Added NPs and cells to printed scaffolds prior to surgical implantation	Improved bone regeneration in rhesus monkey mandibular model	53
PLLA scaffold, tubular and spherical polypyrrole NPs	L929 fibroblasts	Dissolved PLLA in solvent with NPs before printing, then lyophilized printed scaffolds	Inclusion of NPs was minimally cytotoxic; enhanced conductivity	55
PLLA scaffold, CaP NPs, BMP-2 and BSA protein	primary MSCs	PLLA emulsion mixed with CaP NPs and protein solutions before printing on a cryogenic stage, then lyophilized printed scaffolds	Improved compressive strength with addition of CaP NPs; trend of improved attachment and differentiation	59
Poly(ester urea) scaffold, HA nanocrystals	MC3T3-E1 cells	Dissolved poly(ester urea) in solvent with HA nanocrystals before drying and melting into filament, printed filament into scaffolds	Improved cell viability in 30% HA scaffolds; enhanced ALP activity; increased expression of both osteocalcin and bone sialoprotein	60
Alginate gel scaffold, SiO2 NPs	primary MSCs	Mixed NPs with liquid ink before extrusion	Improved compressive modulus and MSC viability; reduced swelling and degradation	61
Alginate gel scaffolds, ZnO NPs	MITC-STO fibroblasts, S. epidermis	Mixed NPs with liquid ink before extrusion	Increased stiffness; antimicrobial properties; no cell toxicity observed	63
PCL scaffold, CNTs	H9C2 myoblast cells	Mixed CNTs with PCL in solvent before printing	Inclusion of CNTs did not impact cell viability; increased elastic modulus conductivity, maximum load, and hardness of scaffolds	45
Methacrylated collagen, alginate, and hybrid scaffolds, CNTs	primary endothelial cells	Mixed CNT solution with liquid ink before printing	Inclusion of CNTs did not impact cell viability; conductivity and mechanical properties were improved	65
PCL/polyethylene oxide scaffold, CNTs	H9C2 myoblast cells	Mixed CNTs with PCL/ polyethylene oxide solution before printing	CNTs decreased cell attachment; cells could still proliferate and align with scaffold	66
PEGDA scaffold, CNTs	neural stem cells	Mixed CNTs with liquid ink before printing	Increased average neurite length; electrical stimulation induced neuronal gene expression	67
PCL scaffold, CNTs	primary MSCs	Mixed CNTs with melted PCL before printing	CNTs improved hardness, elastic modulus, compressive modulus, and viability	68
PPF scaffold, ssDNA/CNT nanocomplexes	MC3T3-E1 cells	Printed PPF scaffolds which were then ammonolyzed and coated with ssDNA-CNT complexes	Toxicity and aggregation of CNTs reduced; increased scaffold	69

Material(s)	Cell Type/ Animal Model	Method	Results	Citation #
			conductivity; enhanced expression of osteogenic markers	
PEEK scaffold, silver NPs, polydopamine coating	MG-63 osteoblast-like cells, E. coli, S. aureus	Sequentially dip-coated with polydopamine and then silver nitrate, followed by UV exposure to form silver NPs	Silver NPs conferred antibacterial activity; slight decrease in cell viability	46
Alginate gel scaffold, iron oxide NPs	primary endothelial cells	Mixed NPs with liquid ink before printing	NPs can be magnetically manipulated within cells and within scaffold; NPs are trackable with μCT	72
PCL scaffold, TiO2 NPs	MC3T3-E1 cells	Mixed NPs with polymer solution before casting in 3DP-derived scaffold cast	Improved mechanical properties; no effect on ALP activity	73
GelMA scaffold, gold NPs	primary MSCs	Mixed NPs with liquid ink before printing	NPs were visible with μCT; no effect on cell viability	74

Table 2:

Summary of materials, methods, and results from studies adding nanoscale features to 3DP scaffolds.

Material(s)	Cell Type/ Animal Model	Method	Results	Citation #
PEG/PEGDA scaffold, HA NPs	primary MSCs	Mixed NPs with liquid ink before casting in 3DP-derived scaffold cast	Increased cell adhesion, cell proliferation, and mechanical properties; indications of enhanced osteogenic differentiation	75
GelMA/PEGDA scaffold, HA and PLGA NPs	primary MSCs	Mixed NPs with liquid ink before printing	Indications of enhanced osteogenic differentiation in scaffolds containing only HA NPs	78
PCL scaffold, HA NPs and microparticles	primary MSCs	Mixed particles with molten polymer to create composite pellets for printing	Incorporating microparticles led to better mechanical properties; only nanoparticle incorporation led to osteogenic differentiation	77
PCL scaffold, PCL micro/nanofibers, alginate/PEO gel	C2C12 myoblast cells	Printed scaffold then electrospun fibers onto the structure	Aligning fibers led to increased myogenic gene expression; improved myoblast morphology	86
PCL, PVA-leached PCL, or PVA-leached collagen scaffold, alginate/PEO/ cell fibers	HUVECs, C2C12 myoblast cells	Printed scaffolds out of PCL, PCL mixed with PVA, or collagen mixed with PVA (PVA groups were incubated in water to remove PVA via leaching), then an alginate/PEO hydrogel containing HUVECs was electrospun over the scaffold	High HUVECs viability after electrospinning; co-culture of HUVECs with seeded C2C12 cells enhanced expression of myogenic genes	87
PCL/PGS/BG scaffold, PCL/PGS fibers	3T3 fibroblast cells	Printed scaffold then electrospun fibers onto one side of the structure	Increased mechanical properties; good biocompatibility	88
Titanium-aluminum-vanadium alloy scaffold	MG-63 osteoblast-like cells	Printed scaffolds which were then blasted with calcium phosphate particles, acid etched with nitric acid, and then had their surfaces pickled with a sodium hydroxide and hydrogen peroxide solution	Differing macroporosities resulted in differing compressive strengths; microscale surface roughness and surface area were equivalent for all macroporosities	89
Titanium-aluminum-vanadium alloy scaffold and surface	primary MSCs	Printed scaffolds blasted with CaP NPs, acid etched with nitric acid, and then had their surfaces pickled with a NaOH and H_2O_2 solution	All textured surfaces had improved osteogenic differentiation; 3D scaffolds had improved osteogenic differentiation over 2D textured surfaces	93
PLA scaffold treated with CAP	primary MSCs, primary fibroblasts, primary osteoblasts	Printed scaffolds treated with CAP for different lengths of time and at different voltages	Reduced contact angle; increased roughness; increased proliferation of MSCs and osteoblasts; increased fibroblast adhesion	94
PVA/MBG scaffold	MC3T3-E1 cells	Mixed MBG with PVA solution before printing, then incubated scaffolds in PBS	Mineralization with PBS increased surface area, roughness, and hardness of scaffolds; enhanced osteogenic gene expression	95

Table 3:

Summary of materials, methods, and results from studies making 3DP scaffolds at the micro and nano scales.

Material	Cell Type/ Animal Model	Method	Results	Citation #
PLLA fiber scaffolds	human smooth muscle cells	Polymer solution was electrospun using stable jet electrospinning onto a movable stage to create aligned fiber scaffolds	Aligned fiber orientations improved cell proliferation and penetration	99
PCL scaffold and PCL fibers	MC3T3-E1 cells, mouse model	Scaffolds were assembled layer by layer through 3DP of macroscale PCL struts followed by pin-modified electrospinning PCL fibers onto the struts for each layer	Increased cell alignment, cell length, and proliferation	100
PCL tube and PCL fibers	human tenocytes	PCL fiber mesh made with EHDP is rolled into a cylinder into which a uniaxially stretched PCL tube is inserted and heat sealed together	Improved elongation, alignment, metabolism, and collagen I expression	102
PCL fibers scaffold and PEDOT:PSS-PEO fibers	H9C2 myoblast cells	PCL microscale fibers were laid down with EHDP, followed by EHDP of PEDOT:PSS-PEO nanofibers to fabricate each layer of the 3D scaffold	Improved conductivity; enhanced cell adhesion, alignment, and coordinated beating of cells	103
PEO fibers	n/a	PEO solution electrospun onto stationary metal line	Can create a walled structure from electrospun polymer	104
PCL/PEG fibers, ROX antibacterial drug	MG-63 osteoblast-like cells, E. coli, S. Aureus	Polymer solution mixed with antibacterial drug, then printed with melt EHDP using a grounded heated cannister and a printing surface with a high voltage applied to it	Bacterial inhibition zones were demonstrated with ROX-loaded scaffolds; minimal impact of scaffolds on cell viability	101
PCL fiber scaffold, chitosan coating	human embryonic stem cells	Polymer solution electrospun onto a movable stage to create walled scaffolds and dip-coated with chitosan solution	Cells were able to attach and proliferate on scaffolds	107
PCL/reduced graphene oxide fiber scaffold	PC-12 neural cells	Polymer solution mixed with reduced graphene oxide then printed into scaffolds with EHDP	Conductive scaffolds had improved cell proliferation and neuronal differentiation	105
PCL/PEO/graphene/ dopamine/gelatin fiber scaffold	PC-12 neural cells	Coaxial nozzles were used in conjunction with EHDP to create scaffolds comprised of PCL/graphene fibers that contained dual cores made from PEO, PEO/dopamine, or PEO/gelatin	Inclusion of dopamine/gelatin improved cell migration	106
Photo polymerizable PLA scaffold	primary rat Schwann cells, SH-SY5Y cells	2PP printed scaffold models were used to make molds that the photopolymerizable PLA was cast in to create final scaffolds	Proliferation was possible on scaffolds; expected morphologies were seen; DNA damage could be mitigated by washing scaffolds with ethanol	111
Modified PLA polymer scaffold	primary MSCs, mouse model	2PP printed scaffolds made from modified PLA molecules	Rougher surfaces; enhanced osteogenic differentiation of cells and calcium deposition in a mouse calvarial model	112
SZ2080 photoresist scaffold	HeLa cancer cell line	Repeated polymer structure patterns were printed with multi-beam 2PP	Higher cell counts in areas with 3D structures; cells seen to interact with polymer scaffold and possibly alter morphology	113
PETA:BisGMA scaffold	primary fibroblast cells	Scaffold was 2PP printed using mixed liquid polymers	Printed micropores fill with cells and ECM; cells differentiated down osteogenic lineage and produced collagen I	114
IP-L780 scaffold	MG-63 osteoblast-like cells	2PP printed scaffolds using a liquid polymer	Layer separation of 2μm to 10μm had best cell penetration; improved osteogenic differentiation	115

Material	Cell Type/ Animal Model	Method	Results	Citation #
Ormocomp scaffold	human neural cells	2PP printed scaffolds using a liquid polymer	Scaffolds allowed directed neurite generation and long term culture	116
PEGDA/hyaluronic acid scaffold	MG-63 osteoblast-like cells, primary fibroblast cells	2PP printed scaffolds made from hyaluronic acid that was modified with acrylate groups and mixed with PEGDA	Scaffolds cytotoxic to fibroblasts but not osteoblast-like cells; inclusion of hyaluronic acid allowed modulation of physical properties	117
GelMA scaffold	primary hLESCs	2PP printed scaffolds using a liquid ink	Observed difference in differentiation of cells based on location in printed structure	118
Polymer scaffold, GelMA and bovine serum albumin membranes	primary chondrocytes	2PP printed polymer scaffolds were made, then membranes of GelMA or bovine serum albumin were printed in a second printing step	Proved protein-polymer hybrid constructs could be printed; pure printed protein structures were lacking in mechanical stability	119
GelMA scaffold	MG-63 osteoblast-like cells	2PP printed scaffolds were generated and cells were mixed with liquid ink before printing	Cells could be incorporated into 2PP printed scaffolds before printing; cell death was not attributed to laser exposure	120
MAPTMS-ZPO-DMAEMA scaffold, BMP-2 protein	primary MSCs	Liquid polymer blend was used to make scaffolds using 2PP printing, after which BMP-2 was either covalently bound or physically adsorbed to the scaffold	BMP-2 addition enhanced osteogenic differentiation, calcium and collagen levels	121
IP-Dip and TiO2 scaffolds, Ti, TiO2, and W coatings	SAOS-2 cells	Liquid polymer was printed into a lattice using 2PP printing, coated with TiO2, Ti/TiO2, or W/TiO2 and then plasma etched (TiO2 group only)	Enhanced actin and mineral deposition on less stiff scaffolds	122
PEGDMA scaffold, rhodamine model drug	primary MSCs, HEK293T cells, induced pluripotent stem cells	2PP printed scaffold using liquid polymer loaded with model drug	Tunable release of model drug; scaffolds were not cytotoxic	123